



## Original Research Article

# Developing a Decision Support Tool for Assessing Land Use Change and BMPs in Large Ungauged Watersheds

Junyu Qi<sup>a</sup>, Sheng Li<sup>a,b</sup>, Charles P.-A. Bourque<sup>a</sup>, Zisheng Xing<sup>a,b</sup>, and Fan-Rui Meng<sup>a,\*</sup>

<sup>a</sup> Faculty of Forestry and Environmental Management, University of New Brunswick,  
P.O. Box 44400, 28 Dineen Drive, Fredericton, NB, E3B 5A3,  
Canada

<sup>b</sup> Potato Research Centre, Agriculture and Agri-Food Canada, P.O. Box 20280, 850  
Lincoln Road, Fredericton, NB, E3B 4Z7, Canada

---

\*Corresponding author: Fan-Rui Meng, Tel.: +1 506 453 4921, E-mail: [fmeng@unb.ca](mailto:fmeng@unb.ca)



1    **Abstract**

2    A simple decision support tool (DST) was developed to evaluate impacts of land use  
3    change and best management practices (BMPs) on water resources for large ungauged  
4    watersheds in New Brunswick, Canada. It was developed based on statistical equations  
5    derived from Soil and Water Assessment Tool (SWAT) simulations applied to a small  
6    experimental watershed in northwest New Brunswick. The DST was subsequently tested  
7    against field measurements and SWAT-model simulations for a larger watershed. Results  
8    from DST reproduced both field data and model simulations of annual stream discharge  
9    and sediment and nutrient loadings fairly well. The relative error of mean annual  
10    discharge and sediment and nutrient loading were within -52 to +27%. Compared with  
11    SWAT, DST has fewer input requirements and can be applied to multiple watersheds  
12    without additional calibration. Also, scenario analyses with DST can be directly  
13    conducted for different combinations of land use and BMPs without complex model  
14    setup procedures.

---

15    **Keywords:** multiple regression; hydrological model; erosion; nitrate leaching;  
16    geographic information system

17

18

19

20

21



## 22        **1. Introduction**

23        Pollution from nonpoint sources poses a significant threat to ecosystems and plant and  
24        animal communities (Vörösmarty et al., 2010). Nonpoint sources of sediment, nutrients,  
25        and pesticides, primarily from agricultural lands, have been identified as major  
26        contributors to water quality degradation (Ongley et al., 2010; Zhang et al., 2004). These  
27        pollutants are difficult to control because they come from many sources (Quan and Yan,  
28        2001). Practices such as strip cropping, terracing, crop rotation, and nutrient management  
29        can be developed to prevent soil erosion and reduce the movement of nutrients and  
30        pesticides from agricultural lands to aquatic ecosystems (D'Arcy and Frost, 2001). These  
31        pollution-prevention methods, known as best management practices (BMPs), are  
32        intended to minimize the negative environmental impact of agricultural activities, while  
33        maintaining land productivity. Reliable information on the impacts of land use change  
34        and BMPs on water quantity and quality is critical to watershed management  
35        (Panagopoulos et al., 2011).

36        Many studies have been conducted to evaluate the impact of land use change and  
37        BMPs on water quality based on field experiments (Novara et al., 2011; Pimentel and  
38        Krummel, 1987; Sadeghi et al., 2012; Turkelboom et al., 1997; Urbonas, 1994).  
39        Monitoring systems have been established to assess the impact of land use change and  
40        BMPs on water resources in order to capture the spatial and temporal variation in soil,  
41        climate, and topographic conditions in watersheds (Veldkamp and Lambin, 2001).  
42        Statistical models developed from field data from small watersheds are usually assumed  
43        to apply to large watersheds (Bloschl and Grayson, 2001; Blöschl and Sivapalan, 1995).  
44        Although it is not difficult to quantify soil erosion and chemical loadings in experimental



45 plots, it is time-consuming and expensive (Mostaghimi et al., 1997). Clearly, it is not  
46 practical to conduct field experiments for every possible combination of land use and  
47 BMPs, under different biophysical conditions. As a result, it is unlikely sufficient field  
48 data could be obtained to develop management plans and conduct cost-benefit analyses.  
49 In addition, statistical models could be potentially derived from experiments; however, it  
50 is difficult to establish cause-and-effect relationships between BMPs and water quality  
51 variables under varied biophysical conditions or to quantify the impact of combined land  
52 use and BMPs on water quality at the watershed scale (Renschler and Lee, 2005).

53 Process-based models of hydrology can be used to extrapolate field data to fill data  
54 gaps (Borah and Bera, 2003; Borah and Bera, 2004; Singh, 1995; Singh and Frevert,  
55 2005; Singh and Woolhiser, 2002). These process-based models provide quantitative  
56 information that is usually difficult to obtain from field experiments (Borah et al., 2002).  
57 For example, ANSWERS (Beasley et al., 1980), CREAMS (Knisel, 1980), GLEAMS  
58 (Leonard et al., 1987), AGNPS (Young et al., 1989), EPIC (Sharpley and Williams,  
59 1990), and SWAT (Arnold et al., 1998) have been used to understand surface runoff, soil  
60 erosion, nutrient leaching, and pollutant-transport processes. However, these process-  
61 based models require extensive input data and complex calibration procedures (Liu et al.,  
62 2015); watersheds with sufficient data to calibrate and validate these models are normally  
63 small, resulting in lack of representation at large spatial scales. Furthermore, once a  
64 model is calibrated, parameters become watershed-specific, which cannot be easily  
65 extended to other watersheds. In addition, these models require specialized expertise,  
66 which prevents non-expert decision makers and economists to use them (Viavattene et al.,  
67 2008).



68 A decision support tool could be developed by combining “decision rules” with  
69 geographic information systems (GIS) for water quality assessment in large ungauged  
70 watersheds. The “decision rules” could be based on regression equations derived from  
71 field experiments (Renschler and Harbor, 2002), or they could be defined simply as  
72 constants based on expert knowledge. Alternatively, simulations from a well-calibrated  
73 hydrological model could be used to develop statistical equation-based “decision rules”.  
74 Apart from defining “decision rules” at each grid cell, to assess water quantity and  
75 quality in streams or at subbasin/watershed outlets, the decision support tool should  
76 consider discharge, sediment, and nutrient routing within the watershed. For example, a  
77 commonly used routing method for sediments is the sediment-delivery ratio (SDR)  
78 method, which is widely employed in many GIS-based erosion models (May and Place,  
79 2010; Wilson et al., 2001; Zhao et al., 2010). For discharge, a simple summation routing  
80 at the outlet produces acceptable accuracy for small- and medium-sized watersheds,  
81 considering that there is negligible water losses from surface runoff and stream flow. For  
82 large watersheds, water losses are generally greater. These water losses can be estimated  
83 using simple linear equations. The annual export of nutrients from watersheds (via the  
84 nutrient-delivery ratio) has been studied empirically in many studies as nutrient loading  
85 per land area (Beaulac and Reckhow, 1982; Endreny and Wood, 2003; Reckhow and  
86 Simpson, 1980).

87 A decision support tool developed based on “decision rules” is generally flexible and  
88 easy for decision makers and economists to use (Endreny and Wood, 2003). However,  
89 their practicality in normal circumstances, particularly with respect to their level of  
90 accuracy, needs to be evaluated. In addition, in order to provide sufficient “decision rules”



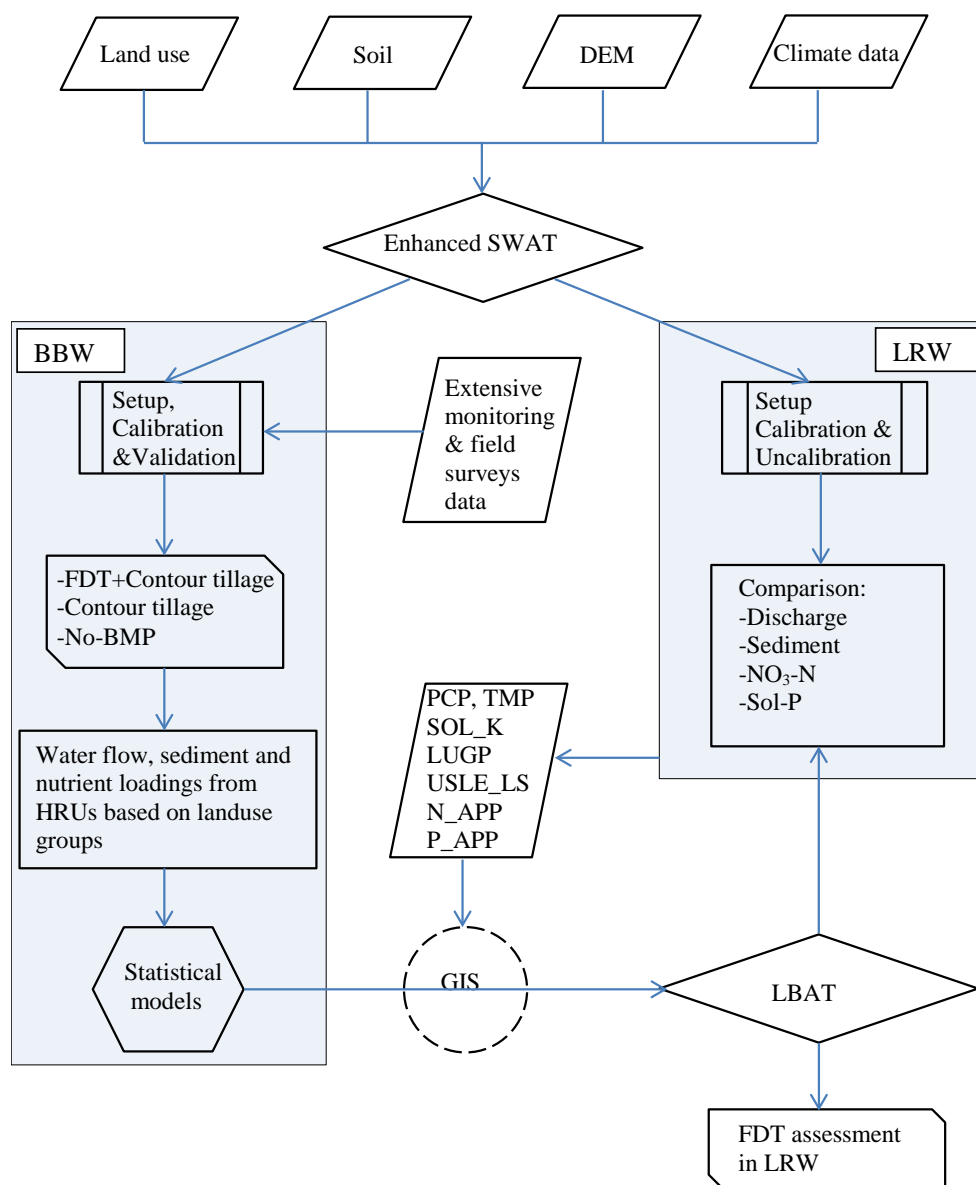
91 with reasonable accuracy, fully validated hydrological models are required to be able to  
92 fill data gaps in field experiments. The present study used the Soil and Water Assessment  
93 Tool (SWAT) to provide modelled data in the development of the decision support tool.  
94 The main objective of the present study is to develop a simple decision support tool with  
95 the intent to evaluate the impact of land use change and BMPs on water resources in a  
96 large ungauged watershed in New Brunswick, Canada. This paper presents the  
97 development and testing of a decision support tool using data from two watersheds in the  
98 potato-belt of New Brunswick; one small experimental watershed, with extensive  
99 monitoring and field survey data, and a larger watershed containing the smaller  
100 watershed.

## 101 **2. Materials and Methods**

102 The general framework of the study is illustrated in Fig. 1. Specifically, this involves:  
103 (1) setting up, calibrating, and validating SWAT for a small experimental watershed; (2)  
104 developing statistical equations based on SWAT-model simulations for different  
105 combinations of land use and BMPs; (3) integrating the statistical equations into a  
106 decision support tool with the aid of ArcGIS; and (4) testing the decision support tool  
107 against field measurements and model simulations of water quantity and quality for a  
108 large watershed.



109



110

111

**Fig. 1** Information flow in development of the decision support tool.



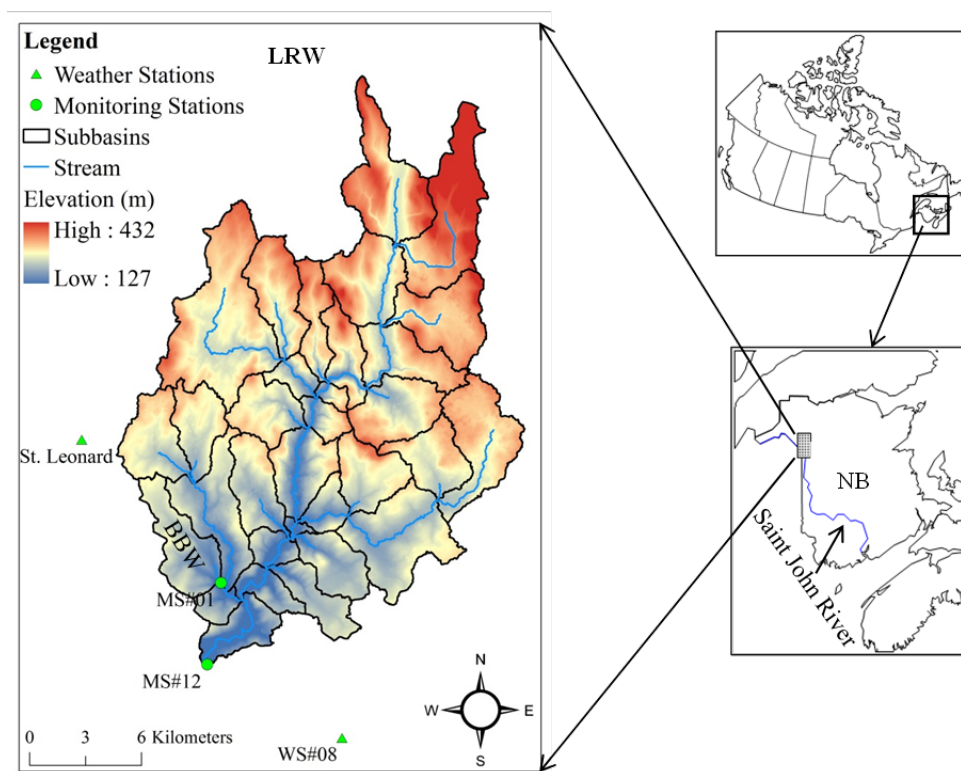
## 112    **2.1 Study Sites and Data Collection**

113        The large watershed of this study is the Little River Watershed (LRW), located in the  
 114    Upper Saint John River Valley of northwestern New Brunswick, Canada (Fig. 2). It  
 115    covers an area approximately 380 km<sup>2</sup> with a mixture of agricultural (16.2%), forest  
 116    (77%), and residential (6.8%) land uses (Xing et al., 2013). Elevation in the watershed  
 117    ranges from 127 to 432 m above mean sea level (Fig. 2). The soil in the study sites is  
 118    classified as mineral, derived from various parent materials. The major associations are  
 119    Caribou, Carleton, Glassville, Grandfalls, Holmesville, McGee, Muniac, Siegas, Thibault,  
 120    Undine, Victoria, Waasis, and one organic soil (Fig. 3). The study site belongs to the  
 121    Upper Saint John River Valley Ecoregion in the Atlantic Maritime Ecozone (Marshall et  
 122    al., 1999). The climate of the region is considered to be moderately cool boreal with  
 123    approximately 120 frost-free days, annually (Yang et al., 2009). The average temperature  
 124    is 3.7°C and annual precipitation is 1037.4 mm (Zhao et al., 2008). About one-third of the  
 125    precipitation is in the form of snow. Snowmelt leads to major surface runoff and  
 126    groundwater recharge events from March to May (Chow and Rees, 2006). The land use  
 127    and soil maps in the setup of SWAT for LRW were derived from publicly available data  
 128    [Energy and Resource Development (ERD), New Brunswick; Fig. 3].





129



130

131 **Fig. 2** Location of the LRW and BBW and water-monitoring stations #01 and #12 as well  
 132 as weather stations #08 and St. Leonard. Elevations and subbasins are also shown for  
 133 LRW.

134

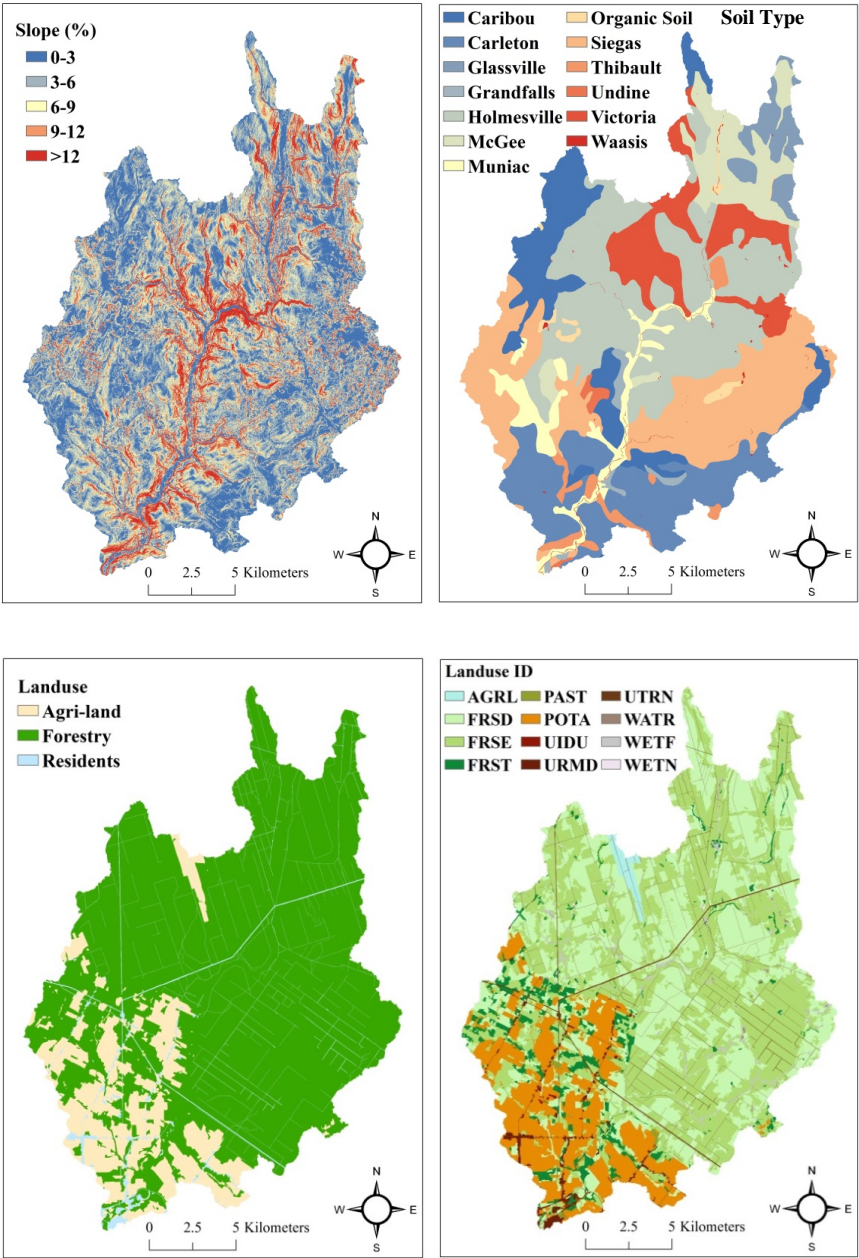


**Fig. 3** Slope classes created using a 10-m resolution LiDAR (Light Detection and Ranging)-based DEM (Digital Elevation Model), soil and land use maps, and land use IDs used by SWAT (see Table 2 for land use ID meaning).



140 The small experimental watershed of the study is the Black Brook Watershed (BBW),  
141 a subbasin of LRW (Fig. 2). The BBW has been studied extensively for more than 20  
142 years to evaluate the impact of agriculture on soil erosion and water quality (Chow and  
143 Rees, 2006; Li et al., 2014). The watershed covers an area of 14.5 km<sup>2</sup>, with 65% being  
144 agriculture land, 21% forest land, and 14% residential areas and wetlands. Slopes vary  
145 from 1-6% in the upper basin to 4-9% in the central area. In the lower portion of the  
146 watershed, slopes are more strongly rolling at 5-16%. Soil surveys (1:10,000 scale)  
147 identified six mineral soils, namely Grandfalls, Holmesville, Interval, Muniac, Siegas,  
148 and Undine, and one organic soil, St. Quentin (Mellerowicz, 1993).

149 A water-monitoring station was established at the outlet of BBW in 1992 (MS#01; Fig.  
150 2) and another (MS#12) at the outlet of LRW in 2001. At these stations, V-notch weirs  
151 were installed, and the stage height of the water was recorded using a Campbell-  
152 Scientific CR10X data logger. Stage height values were converted to total flow rates with  
153 a calibration curve function (Chow et al., 2011). Water samples were collected with an  
154 ISCO automatic sampler. Sampling frequency was set at one sample every 72 hours when  
155 runoff was absent. During runoff events, sampling frequency was increased to one  
156 sample every 5-cm change in stage height. Samples were analyzed for concentration of  
157 suspended solids, nitrate-nitrogen (NO<sub>3</sub>-N), and soluble-phosphorus (Sol-P). Detailed  
158 description of data collection procedures and sample analyses can be found in Chow et al.  
159 (2011). Weather data including daily precipitation, air temperature, relative humidity, and  
160 wind speed were acquired from the St. Leonard Environment Canada weather station,  
161 located approximately 5 km northwest of BBW (Fig. 2). The daily average relative  
162 humidity and wind speed were calculated based on hourly values. Since this weather



station did not monitor daily solar radiation, the study used solar radiation collected from a weather station located approximately 10 km southeast of BBW (WS#08; Fig. 2).

## 2.2 Modification of SWAT

As a process-based semi-distributed watershed model, SWAT is designed to simulate hydrological processes and predict water quantity and quality as affected by land use, land management practices, and climate change (Arnold et al., 1998). It provides a flexible framework that allows for simulations of the impact of a broad range of BMPs, such as crop cover, filter strips, conservation tillage, irrigation, and flood-prevention structures (Gassman et al., 2005; Ullrich and Volk, 2009). The SWAT-model is currently one of the most commonly used hydrological models to study nonpoint source pollution problems (Behera and Panda, 2006) and evaluate the impact of BMPs on water quantity and quality at various spatial scales (Gassman et al., 2005).

Many studies have used SWAT as a decision support tool to evaluate water resources in large ungauged watersheds. It is believed that SWAT is able to provide reliable evaluations even without calibration. SWAT analyzes hydrological processes for watersheds by discretizing them into subbasins, which are then themselves subdivided into hydrological response units (HRUs) of homogeneous land use, soil properties, and slope (Yan et al., 2013; Yang et al., 2009). The model calculates the water balance, crop growth, nutrient cycling, and pesticide movement at the HRU level. Water flow and sediment and nutrient transport from each HRU are summed and the resulting loadings are then routed by means of channels, ponds, and reservoirs to the watershed outlet. Model outputs include HRU-, subbasin-, and watershed-level values of surface, lateral, and base flows, as well as sediment and nutrient loadings.



186 In Atlantic Canada, where substantial snow accumulates, SWAT-predicted soil  
 187 temperatures have been found to disagree with field measurements (Yang et al., 2009),  
 188 especially in winter. To address this discrepancy new physically-based soil-temperature  
 189 and snowmelt modules were previously developed for SWAT to account for snow-  
 190 insulation effects (Qi et al., 2016a, b) and rain-on-snow events (Qi et al., 2017a). Further  
 191 modification to SWAT included a modification to the universal soil loss equation  
 192 (MUSLE) by introducing a variable soil erodibility coefficient (K-factor) to address  
 193 effects of freeze-thaw cycles on erosion in cold regions (Qi et al. 2017b). The following  
 194 changes to SWAT have improved the overall accuracy of the simulations when tested  
 195 against field measurements.

### 196 **2.3 SWAT Setup, Calibration, and Validation for BBW and LRW**

197 The new SWAT model has been subsequently set up, calibrated, and validated for  
 198 BBW as reported in Qi et al. (2017b). Specific model inputs for both watersheds are  
 199 provided in Table 1. The same weather data were used for both watersheds (Table 1). The  
 200 Digital Elevation Model (DEM) for LRW and BBW (Qi et al., 2017b) were both based  
 201 on high resolution LiDAR (Light Detection and Ranging) data, the first was created at  
 202 10-m and the second, at 1-m resolution (Qi et al., 2017b). The LRW was delineated into  
 203 32 subbasins from which their topographic characteristics were defined (Fig. 2). The soil  
 204 types and slopes, which were classified into five separate classes, are illustrated in Fig. 3  
 205 for LRW. After combining the soil, slope, and land use maps through the ArcSWAT-  
 206 interface function, 362 HRUs were subsequently created for LRW.

207  
 208



209 **Table 1** Datasets in SWAT setup, calibration, and validation for BBW and LRW.

Dataset	BBW	LRW
LiDAR DEM resolution	1-m	10-m
Soil map	Survey (1993)	ERD
Land use maps	Survey (92-11)	ERD (one map)
Precipitation, temperature, relative humidity & wind speed	St. Leonard (92-11)	St. Leonard (01-10)
Solar radiation	WS#08 (92-11)	WS#08 (01-10)
Contour tillage operation (spring and fall)	Survey (92-11)	Only for potato and barley (01-10)
Fertilizer application	Survey (92-11)	Estimated from BBW (2001)
Crop rotation	Survey (92-11)	Potato-barley (01-10)
Terraces and grassed waterways	Survey (92-11)	Negligible
Discharge, sediment, NO <sub>3</sub> -N and Sol-P	MS#01 (92-11)	MS#12 (01-10)

210

211

212 Since only one land use map was available for LRW (Table 1), assumptions were  
 213 made based on information available on land use and management records for BBW to  
 214 adjust the SWAT-management files for LRW as follows:

215 (1) Potato-barley rotations were assigned to the land use ID POTA (Table 2); for other  
 216 land use IDs, a single crop was considered;

217 (2) Fertilizers were applied only to potato and barley fields, and fertilizer amounts and  
 218 N:P (nitrogen-to-phosphorus) ratios were averaged for potato and barley fields over the  
 219 entire watershed, based on 2001 survey data from BBW;

220 (3) Contour tillage was applied only to potato and barley fields;

221 (4) Flow diversion terraces (FDT) and grassed waterways in LRW were assumed not  
 222 used. It is worth noting that these four assumptions serve as a baseline scenario for the  
 223 assessment of FDT in LRW at a later time.

224 In order to evaluate the global performance of the decision support tool for LRW,  
 225 related land use and management files were prepared and accessed by SWAT. For



226 purpose of comparison, simulations with SWAT were produced in an initial application  
 227 by setting the adjustable parameters of the model to their default values, and in a second  
 228 application by setting the parameters according to values produced with a watershed-  
 229 specific model calibration to BBW. This approach with model parameterization is widely  
 230 accepted when applying SWAT to large ungauged watersheds (Panagopoulos et al.,  
 231 2011).

## 232 **2.4 Decision Rules**

233 The decision support tool was designed to use the “decision rules” to estimate annual  
 234 discharge and sediment and nutrient loadings from individual grid cells:

$$236 \quad A = \sum_{i=1}^n DR_i \cdot A_i, \quad (1)$$

237  
 238 where  $A$  is the annual discharge or sediment and nutrient loadings at the outlet of the  
 239 watershed,  $DR_i$  and  $A_i$  are the delivery ratios and annual discharge or loadings,  
 240 respectively, for grid cell  $i$ . For the present study, statistical equations derived from  
 241 simulations of the calibrated version of the enhanced SWAT-model for BBW (Qi et al.,  
 242 2017b) were defined as the “decision rules” in the decision support tool.

### 243 **2.4.1 Land Use Groups and BMP Scenarios**

244 In statistical equation development, land use in BBW (24, in total) was first classified  
 245 into five land use classes according to their influences on hydrological processes (Table  
 246 2). Note that WATR was not used due to its small overall coverage (Fig. 3). As for  
 247 watershed management, we considered three main BMPs, i.e.,





- 248 (1) FDT + contour tillage;  
 249 (2) Contour tillage; and  
 250 (3) No-BMP (without FDT and contour tillage).

251

252 **Table 2** Land use and land use groups (LUGP) for BBW and LRW.

LUGP	Land use ID in SWAT	Land use type
AGRL (General crops)	AGRL	Agricultural Land-Generic
	CANA	Canola
	CRON	Corn
	FPEA	Field peas
	POTA	Potato
GRAN (Grains)	BARL	Barley
	OATS	Oats
	PMIL	Millet
	RYE	Rye
	SWHT	Spring wheat
	WWHT	Winter wheat
GRAS (Grasses)	BERM	Bermuda grass
	CLVR	Clover
	HAY	Hay
	PAST	Past
	RYEG	Ryegrass
	TIMO	Timothy
FORT (Forestry)	FRSD	Forest-Deciduous
	FRSE	Forest-Evergreen
	FRST	Forest-Mixed
	RNGB	Range-Bush
	WETF	Wetlands-Forested
	WETN*	Wetlands-No-Forest
NOCR (Non-vegetated lands)	URMD	Residential
	UTRN	Transportation
	UIDU*	Industrial

Note: “\*” indicates unique land use types to LRW not present in BBW and, therefore, unaccounted for in the development of the decision support tool.

253

254 The calibrated version of the enhanced SWAT-model for BBW was used to generate  
 255 annual outputs based on HRUs from 1992 to 2011. The model was ran three times to  
 256 generate the BMP-specific data for statistical equation development.





## 2.4.2 Explanatory Variables Selection

Explanatory candidate variables must be physically-meaningful in hydrological and biochemical processes. It is worth noting that both continuous and categorical variables were included in the regression equation. The land use group (LUGP) was the only categorical variable, and the remaining were all continuous variables. To detect significant predictors, the analysis of covariance (ANCOVA) was used. It requires at least one continuous and one categorical explanatory variable and is used to identify the major and interaction of predictor variables. By including continuous variables, the method can reduce the variance of error to increase the statistical power and precision in estimating categorical variables (Keselman et al., 1998; Li et al., 2014). Inclusion of interaction terms in these regression models dramatically increased model performance.

In the present study, we only considered interactions between two explanatory variables at a time. Student t-tests were conducted to examine the statistical significance of each level of LUGP and their interaction with the various continuous variables. When one level of LUGP (e.g., GRAN; Table 2) did not significantly correlate with water quality or quantity, or there were nominal interactions between a given level and other explanatory variables, this particular level of LUGP would be combined with other levels of LUGP until all new levels of LUGP were statistically significant.

Multiple linear regression analyses were used to relate annual total discharge (mm) and sediment ( $\text{t ha}^{-1}$ ),  $\text{NO}_3\text{-N}$  ( $\text{kg ha}^{-1}$ ), and Sol-P ( $\text{kg ha}^{-1}$ ) loadings to the explanatory variables. These work was conducted in R (Ihaka and Gentleman, 1996). Only six continuous explanatory variables were determined for the specification of the statistical models. Annual precipitation (PCP), annual mean air temperature (TMP), and mean



280 saturated hydraulic conductivity of soil (SOL\_K) were common to the dependent  
 281 variables (i.e., total discharge and sediment, NO<sub>3</sub>-N, and Sol-P loadings). The LS-factor  
 282 (USLE\_LS) and annual N and P application rates (N\_APP and P\_APP) were unique to  
 283 the equations addressing sediment, NO<sub>3</sub>-N, and Sol-P loading.

### 284 2.4.3 Delivery Ratio Definition

285 The LS-factor of the universal soil loss equation (USLE) was determined by slope  
 286 gradient ( $slp$ ) and slope length ( $L$ ) of individual HRUs:

$$288 \text{USLE\_LS} = \left\{ \frac{L}{22.1} \right\}^m \cdot (65.41 \cdot \sin^2(a) + 4.56 \cdot \sin(a) + 0.065) \quad (2)$$

289  
 290 where  $m$  is the equation exponent and  $a$  is the angle of the slope (in degrees). The  
 291 exponent  $m$  is calculated by,

$$293 m = 0.6 \cdot (1 - \exp[-35.835 \cdot slp]) \quad (3)$$

294  
 295 where  $slp$  is in units of  $\text{m m}^{-1}$ . For the decision support tool, slope length  $L$  equals to the  
 296 length of the grid side and slope gradient was determined by the *Slope* tool in ArcGIS.  
 297 The sediment-delivery ratio was not considered in the decision support tool application to  
 298 BBW. We assumed that annual sediment loadings from grid cells in decision support tool  
 299 were all exported to the outlet of BBW. However, when the decision support tool was  
 300 applied to LRW, the sediment-delivery ratio was used to correct estimates of sediment  
 301 loading at the watershed outlet. The sediment loadings at the outlet of LRW ( $sed$ ) were  
 302 determined by



303

$$304 \quad sed = SDR \cdot sed^{\sim} \quad (4)$$

305

306 where  $sed^{\sim}$  is the sediment loading calculated with the sediment loading equation (one for  
 307 each BMP and land use group), and  $SDR$  is determined by (Vanoni, 1975)

308

$$309 \quad SDR = 0.37 \cdot D^{-0.125} \quad (5)$$

310

311 where  $D$  ( $\text{km}^2$ ) is the drainage area. For annual discharge and nutrient loadings, we  
 312 assumed their delivery ratios equal to 1.0 for all grid cells in LRW.

## 313 **2.5 Decision Support Tool Assessment (LBAT)**

314 Inputs to the decision support tool included the six continuous explanatory variables  
 315 and LUGP as well as information on management practices, e.g., contour tillage and FDT  
 316 implementation. Simulations from each grid cells were summarized at the outlet of the  
 317 study watersheds. We first tested the impact of cell size on simulations of water quantity  
 318 and quality at the outlet of BBW. The cell size range was determined by considering  
 319 different farmland sizes in the watershed. We assumed that farmland-based grid cells can  
 320 sufficiently represent basic hydrological processes, land use change, and management  
 321 practice implementations for hydrological modeling. Simulated annual water flow and  
 322 sediment and nutrient loadings with the decision support tool were compared with those  
 323 produced with the calibrated version of the enhanced SWAT-model. Subsequently, the  
 324 decision support tool was applied to LRW, and the simulations were compared with the  
 325 results of the uncalibrated and calibrated versions of SWAT. The purpose of this was to



test if the decision support tool (i.e., land use and BMP assessment tool; LBAT) performed better, or at least as well, as both the uncalibrated and calibrated version of SWAT.

Model performance in terms of water quantity and quality at the outlet of the study watersheds was assessed based on the coefficient of determination ( $R^2$ ) and relative error (Re), i.e.,

$$R^2 = \left( \frac{\sum_{i=1}^n (O_i - O_{avg}) \cdot (P_i - P_{avg})}{\left[ \sum_{i=1}^n (O_i - O_{avg})^2 \cdot \sum_{i=1}^n (P_i - P_{avg})^2 \right]^{0.5}} \right)^2 \quad (6)$$

$$Re = \frac{(P_{avg} - O_{avg})}{O_{avg}} \cdot 100\% \quad (7)$$

where  $O_i$ ,  $P_i$ ,  $O_{avg}$ , and  $P_{avg}$  are the observed and predicted and averages of the observed and predicted values, respectively.

## 2.6 FDT Assessment in LRW

A series of FDT-implementation scenarios were set up for LBAT based on six slope classes to assess the impact of FDT on water quantity and quality on agricultural lands in LRW (Fig. 3; Table 3). From scenarios one (S1) to six (S6), total area protected by FDT gradually increased until all agricultural lands were protected (Table 3). Mean annual simulations of total discharge and sediment,  $\text{NO}_3\text{-N}$ , and Sol-P loadings from LRW from 2001 to 2010 were compared with those of the baseline scenario (FDT = 0%) for each



346 scenario using two performance indicators, i.e., mean difference (MD) and % relative  
 347 difference (PRD), given as:

348 (1) MD = output with FDT – output without FDT, and

349 (2) PRD (%) = MD/output without FDT × 100.

350 (3)

351 **Table 3** Slope classes and corresponding areas in the agricultural land of LRW.

Scenario	Slope	Area protected by FDT (ha)	Agricultural lands (%)
S1	≥5%	624	10
S2	≥4%	1328	22
S3	≥3%	2224	37
S4	≥2%	3680	61
S5	≥1%	5360	89
S6	≥0	6048	100

352

### 353 3. Results and Discussion

#### 354 3.1 Statistical Equations (Decision Rules)

##### 355 3.1.1 Model Structure and Coefficients

356 Linear regression equations and their explanatory variables for annual discharge and  
 357 sediment, NO<sub>3</sub>-N, and Sol-P loadings under different combinations of land use groups  
 358 and BMP scenarios are provided in Tables 4 and 5. In total, three discharge models (Dis1,  
 359 Dis2, and Dis3) and five sediment (Sed1\_1, Sed1\_2, Sed1\_3, Sed2, and Sed3), NO<sub>3</sub>-N  
 360 (N1\_1, N1\_2, N1\_3, N2, and N3), and Sol-P (P1\_1, P1\_2, P1\_3, P2, and P3) loading  
 361 models were developed. Data transformations (via logarithm and power transformations)  
 362 were applied to sediment, NO<sub>3</sub>-N, and Sol-P loadings to meet the assumption of  
 363 normality in multiple regression analysis (Table 4). The contour tillage and FDT were  
 364 applied only to agricultural lands, including land use groups AGRL, GRAN, and GRAS



365 (Table 4). For the no-BMP scenario, three separate sediment, NO<sub>3</sub>-N, and Sol-P loading  
366 models were developed for agricultural lands (AGRL, GRAN, and GRAS), non-  
367 vegetated lands (NOCR), and forest lands (FORT), and one discharge model (Dis1) for  
368 all land use groups (Table 4). It is worth noting that the sediment loading model, Sed3,  
369 was a modified version of Sed1\_1 (multiplied by TERR\_P) for the FDT + contour tillage  
370 scenario (Table 4), and the values of TERR\_P (Qi et al., 2017b) used for Sed3 were the  
371 same as the calibrated values in SWAT for BBW (Qi et al., 2017b). Also, NO<sub>3</sub>-N and  
372 Sol-P loadings (N1\_2 and P1\_2) for non-vegetated lands (NOCR) were determined as  
373 constants, which were equal to the calculated means of NO<sub>3</sub>-N and Sol-P loadings  
374 determined by SWAT (i.e., 24 and 0.61 kg ha<sup>-1</sup>, respectively; Table 4).

375 As for LUGP (including AGRL, GRAN, GRAS, FORT, and NOCR; Table 2), three  
376 new land use groups (i.e., LUGP1, LUGP2, and LUGP3) were formulated by combining  
377 agricultural lands AGRL, GRAN, and GRAS during model development (Tables 4 and 5).  
378 For example, LUGP2 was derived by combining AGRL, GRAN, and GRAS on total  
379 discharge (i.e., Dis1 model). Individual model structures are shown in Table 4, whereas  
380 the explanatory variables for these models appear in Tables 6, 7, 8 and 9. The coefficients  
381 estimated for the explanatory variables and their interactions, and their t-test results are  
382 also shown. Most of the *p*-values for these explanatory variables were < 0.001, except for  
383 several that were between 0.001 and 0.08, which were also taken as acceptable.



**Table 4** Statistical models based on land use groups (LUGP) and BMPs.

BMPs	LUGP*	Model	Structure
No-BMP	CRGP2,NOCR,FORT	Dis1	Discharge = $f(\text{PCP, TMP, SOL\_K, LUGP2})$
Contour tillage	AGRL,GRAN,GRAS	Dis2	= $f(\text{PCP, TMP, SOL\_K})$
FDT+Contour tillage	AGRL,GRAN,GRAS	Dis3	= $f(\text{PCP, TMP, SOL\_K})$
No-BMP	CRGP1,GRAS	Sed1_1	Sediment <sup>(U/10)</sup> = $f(\text{USLE\_LS, PCP, TMP, SOL\_K, LUGP1})$
	NOCR	Sed1_2	= $f(\text{USLE\_LS, PCP})$
	FORT	Sed1_3	= $f(\text{USLE\_LS, PCP, SOL\_K})$
Contour tillage	CRGP1,GRAS	Sed2	Sediment <sup>(U/10)</sup> = $f(\text{USLE\_LS, PCP, TMP, SOL\_K, LUGP1})$
FDT+Contour tillage	AGRL,GRAN,GRAS	Sed3	Sediment = $\text{Sed1\_1} \times \text{TERR\_P}$
No-BMP	AGRL,GRAN,GRAS	N1_1	$\text{Log}(\text{NO}_3\text{-N}) = f(\text{N\_APP, PCP, TMP, SOL\_K, LUGP})$
	NOCR	N1_2**	$\text{NO}_3\text{-N} = 24 \text{ kg ha}^{-1}$
	FORT	N1_3	$\text{Log}(\text{NO}_3\text{-N}) = f(\text{PCP, TMP, SOL\_K})$
Contour tillage	AGRL,GRAN,GRAS	N2	$\text{Log}(\text{NO}_3\text{-N}) = f(\text{N\_APP, PCP, TMP, SOL\_K, LUGP})$
FDT+Contour tillage	CRGP3,GRAN	N3	= $f(\text{N\_APP, PCP, TMP, SOL\_K, LUGP3})$
No-BMP	CRGP1,GRAS	P1_1	$\text{Log}(\text{Sol-P}) = f(\text{P\_APP, PCP, TMP, SOL\_K, LUGP1})$
	NOCR	P1_2**	$\text{Sol-P} = 0.61 \text{ kg ha}^{-1}$
	FORT	P1_3	$\text{Log}(\text{Sol-P}) = f(\text{PCP, TMP, SOL\_K})$
Contour tillage	CRGP1,GRAS	P2	$\text{Log}(\text{Sol-P}) = f(\text{P\_APP, PCP, TMP, SOL\_K, LUGP1})$
FDT+Contour tillage	AGRL,GRAN,GRAS	P3	= $f(\text{P\_APP, PCP, TMP, SOL\_K, LUGP})$

\*AGRL and GRAN are combined into one group, namely CRGP1 in LUGP1; AGRL, GRAN and GRAS are combined into one group, namely CRGP2 in LUGP2; AGRL and GRAS are combined into one group, namely CRGP3 in LUGP3; \*\* variable is set constant.



**Table 5** Explanatory variables determined for statistical analysis.

Variable	Unit	Meaning
LUGP	—	Land use groups including AGRL, GRAN, GRAS, FORT, and NOCR
LUGP1	—	AGRL and GRAN are combined into a new group, CRGP1
LUGP2	—	AGRL, GRAN, and GRAS are combined into a new group, CRGP2
LUGP3	—	AGRL and GRAS are combined into a new group, CRGP3
N_APP	kg ha <sup>-1</sup>	Annual N application rate
P_APP	kg ha <sup>-1</sup>	Annual P application rate
PCP	mm	Annual precipitation
SOL_K	mm h <sup>-1</sup>	Mean saturated hydraulic conductivity of soil
TERR_P	—	P-factor for FDT
TMP	°C	Annual mean air temperature
USLE_LS	—	LS-factor of USLE





405

406 **Table 6** Coefficient values for the three discharge models corresponding to land use and

407 BMPs described in Table 4.

Model variable	Estimate	Std. Error	t-value	p-value
<b>Dis1</b>				
Intercept	-1565	24.04	-65.089	<0.001
PCP	1.933	0.02176	88.837	<0.001
TMP	282.7	6.091	46.402	<0.001
SOL_K	0.06338	0.00992	6.389	<0.001
FORT	30.79	14.16	2.175	0.030
NOCR	162.2	14.51	11.181	<0.001
PCP:TMP	-0.2488	0.005487	-45.352	<0.001
PCP:FORT	0.04684	0.01191	3.934	<0.001
PCP:NOCR	-0.0535	0.01224	-4.37	<0.001
TMP:FORT	9.723	1.684	5.775	<0.001
TMP:NOCR	4.506	1.731	2.603	0.009
SOL_K:FORT	-0.3769	0.03403	-11.076	<0.001
SOL_K:NOCR	-0.2959	0.032	-9.248	<0.001
<b>Dis2</b>				
Intercept	-1633	27.29	-59.84	<0.001
PCP	1.995	0.02472	80.69	<0.001
TMP	302.2	6.87	43.98	<0.001
SOL_K	0.08696	0.01167	7.45	<0.001
PCP:TMP	-0.2662	0.006199	-42.94	<0.001
<b>Dis3</b>				
Intercept	-1666	36.58	-45.54	<0.001
PCP	2.007	0.03305	60.713	<0.001
TMP	298	9.351	31.865	<0.001
SOL_K	0.09353	0.01573	5.946	<0.001
PCP:TMP	-0.2606	0.008406	-31.004	<0.001

408

409

410

411

412

413



**Table 7** Coefficient values for the four sediment loading models corresponding to land use and BMPs described in Table 4.

Model variable	Estimate	Std. Error	t-value	p-value
<b>Sed1_1</b>				
Intercept	0.2749	0.06125	4.488	<0.001
USLE_LS	0.1201	0.02224	54.018	<0.001
PCP	0.000788	5.54E-05	14.218	<0.001
TMP	0.1117	0.01528	7.307	<0.001
SOL_K	0.000568	0.00022	2.585	0.010
GRAS	-0.0353	0.00881	-4.007	<0.001
USLE_LS:SOL_K	-0.00014	4.69E-05	-3.045	0.002
USLE_LS:GRAS	-0.02623	0.006826	-3.842	<0.001
PCP:TMP	-0.00011	1.38E-05	-7.967	<0.001
PCP:SOL_K	-4.6E-07	1.91E-07	-2.406	0.016
<b>Sed1_2</b>				
Intercept	0.8575	0.008826	97.15	<0.001
PCP	0.000123	7.82E-06	15.67	<0.001
PCP:USLE_LS	0.000209	5.02E-06	41.65	<0.001
<b>Sed1_3</b>				
(Intercept)	0.3992	0.02267	17.613	<0.001
USLE_LS	0.07935	0.01967	4.034	<0.001
PCP	0.000204	1.96E-05	10.371	<0.001
SOL_K	0.000545	5.71E-05	9.534	<0.001
USLE_LS:PCP	4.94E-05	1.71E-05	2.9	0.004
USLE_LS:SOL_K	-0.00067	4.89E-05	-13.718	<0.001
<b>Sed2</b>				
Intercept	0.2591	0.05228	4.956	<0.001
USLE_LS	0.12	0.001898	63.218	<0.001
PCP	0.000767	4.73E-05	16.212	<0.001
TMP	0.1162	0.01304	8.907	<0.001
SOL_K	0.000746	0.000188	3.981	<0.001
GRAS	-0.06937	0.01648	-4.211	<0.001
USLE_LS:SOL_K	-0.00013	4E-05	-3.137	0.002
USLE_LS:GRAS	-0.02662	0.005829	-4.567	<0.001
PCP:TMP	-0.00011	1.18E-05	-9.522	<0.001
PCP:SOL_K	-6.3E-07	1.63E-07	-3.846	<0.001
TMP:GRAS	0.007415	0.003664	2.024	0.043



418

419 **Table 8** Coefficient values for the four NO<sub>3</sub>-N loading models corresponding to land use

420 and BMPs described in Table 4.

Model variable	Estimate	Std. Error	t-value	p-value
<b>N1_1</b>				
Intercept	1.44	0.1753	8.213	<0.001
N_APP	-0.00862	0.000699	-12.325	<0.001
PCP	0.000543	0.00016	3.4	<0.001
TMP	0.1363	0.03357	4.059	<0.001
SOL_K	-0.00344	9.78E-05	-35.163	<0.001
GRAN	-1.117	0.1021	-10.937	<0.001
GRAS	-1.97	0.1562	-12.611	<0.001
N_APP:PCP	5.31E-06	6.45E-07	8.233	<0.001
N_APP:TMP	0.000963	7.45E-05	12.929	<0.001
N_APP:SOL_K	9.6E-06	6.4E-07	15.024	<0.001
PCP:GRAN	0.000677	9.38E-05	7.215	<0.001
PCP:GRAS	0.001029	0.000143	7.201	<0.001
PCP:TMP	-0.00025	2.64E-05	-9.467	<0.001
TMP:GRAN	0.1	0.01134	8.817	<0.001
TMP:GRAS	0.2132	0.01651	12.912	<0.001
<b>N1_3</b>				
Intercept	-1.411	0.3087	-4.573	<0.001
PCP	0.001875	0.000279	6.710	<0.001
TMP	0.4437	0.07831	5.666	<0.001
SOL_K	-0.00104	0.000116	-8.979	<0.001
PCP:TMP	-0.00032	7.06E-05	-4.484	<0.001
<b>N2</b>				
Intercept	1.429	0.1757	8.134	<0.001
N_APP	-0.00858	0.000701	-12.233	<0.001
PCP	0.000548	0.00016	3.425	<0.001
TMP	0.1376	0.03365	4.089	<0.001
SOL_K	-0.00345	9.8E-05	-35.223	<0.001
GRAN	-1.11	0.1023	-10.849	<0.001
GRAS	-1.962	0.1566	-12.526	<0.001
N_APP:PCP	5.3E-06	6.47E-07	8.187	<0.001
N_APP:TMP	0.000957	7.46E-05	12.82	<0.001
N_APP:SOL_K	9.65E-06	6.4E-07	15.067	<0.001
PCP:GRAN	0.000674	9.41E-05	7.167	<0.001
PCP:GRAS	0.001026	0.000143	7.162	<0.001
PCP:TMP	-0.00025	2.64E-05	-9.456	<0.001



TMP:GRAN	0.09934	0.01137	8.738	<0.001
TMP:GRAS	0.2122	0.01655	12.821	<0.001
<b>N3</b>				
Intercept	-0.3595	0.1718	-2.092	0.037
N_APP	-0.00131	0.000435	-3.011	0.003
PCP	0.001621	0.00015	10.806	<0.001
TMP	0.3977	0.03857	10.312	<0.001
SOL_K	-0.00386	0.000505	-7.641	<0.001
GRAN	-0.2133	0.07504	-2.842	0.005
N_APP:PCP	1.65E-06	3.59E-07	4.61	<0.001
N_APP:TMP	0.000281	4.74E-05	5.939	<0.001
N_APP:GRAN	0.000716	0.000292	2.453	0.014
PCP:TMP	-0.00035	3.32E-05	-10.506	<0.001
PCP:SOL_K	1.21E-06	4.36E-07	2.781	0.005
PCP:GRAN	0.000267	5.82E-05	4.577	<0.001
TMP:GRAN	-0.04685	0.008004	-5.853	<0.001

421

422

423

424

425

426

427

428

429

430

431

432

433

434

435



**Table 9** Coefficient values for four Sol-P models corresponding to land use and BMPs described in Table 4.

Model variable	Estimate	Std. Error	t-value	p-value
<b>P1_1</b>				
Intercept	-3.711	0.1306	-28.416	<0.001
P_APP	0.002341	0.000623	3.757	<0.001
PCP	0.003195	0.000117	27.286	<0.001
TMP	0.5542	0.03197	17.337	<0.001
SOL_K	0.00298	0.000472	6.305	<0.001
GRAS	-0.4321	0.0382	-11.312	<0.001
P_APP:PCP	-2.4E-06	5.2E-07	-4.64	<0.001
P_APP:TMP	0.000829	7.7E-05	10.797	<0.001
PCP:TMP	-0.00052	2.9E-05	-18.297	<0.001
PCP:SOL_K	-1.2E-06	3.97E-07	-3.095	0.002
TMP:SOL_K	-0.00026	5.7E-05	-4.526	<0.001
TMP:GRAS	0.03787	0.00941	4.024	<0.001
<b>P1_3</b>				
Intercept	-4.43817	0.589848	-7.512	<0.001
PCP	0.002509	0.000534	4.701	<0.001
TMP	0.417306	0.1496445	2.789	0.005
SOL_K	0.001247	0.000222	5.622	<0.001
PCP:TMP	-0.0003	0.000135	-2.253	0.024
<b>P2</b>				
Intercept	-3.667	0.1357	-27.017	<0.001
P_APP	0.003461	0.000663	5.218	<0.001
PCP	0.003017	0.000122	24.783	<0.001
TMP	0.5149	0.03304	15.584	<0.001
SOL_K	0.003531	0.000488	7.233	<0.001
GRAS	-0.2039	0.09001	-2.265	0.024
P_APP:PCP	-2.4E-06	5.54E-07	-4.305	<0.001
P_APP:TMP	0.000432	7.93E-05	5.445	<0.001
P_APP:GRAS	-0.03304	0.007019	-4.707	<0.001
PCP:TMP	-0.00044	2.95E-05	-14.952	<0.001
PCP:SOL_K	-1.4E-06	4.1E-07	-3.446	<0.001
PCP:GRAS	-0.00025	7.66E-05	-3.25	0.001
TMP:SOL_K	-0.00025	5.87E-05	-4.184	<0.001
TMP:GRAS	0.05117	0.009839	5.201	<0.001
<b>P3</b>				
Intercept	-2.817	0.2548	-11.054	<0.001
P_APP	-0.01363	0.001854	-7.352	<0.001
PCP	0.002778	0.000178	15.609	<0.001



TMP	0.1406	0.06523	2.155	0.031
SOL_K	0.00651	0.000702	9.279	<0.001
GRAN	-0.9386	0.1378	-6.812	<0.001
GRAS	-0.9931	0.1813	-5.478	<0.001
P_APP:TMP	0.003562	0.000491	7.252	<0.001
P_APP:GRAN	0.007736	0.002179	3.549	<0.001
P_APP:GRAS	-0.05489	0.01295	-4.24	<0.001
PCP:TMP	-0.0003	4.42E-05	-6.763	<0.001
PCP:SOL_K	-3.7E-06	5.78E-07	-6.359	<0.001
PCP:GRAN	0.000112	5.1E-05	2.192	0.028
PCP:GRAS	-0.00019	0.000109	-1.74	0.082
TMP:SOL_K	-0.00021	8.8E-05	-2.4	0.016
TMP:GRAN	0.1798	0.03332	5.397	<0.001
TMP:GRAS	0.247	0.03581	6.898	<0.001

438

### 439 3.1.2 Statistical Equation Assessment

440 Simulations based on the statistical equations and the calculated outputs from  
 441 individual HRUs for the different BMPs are compared in Table 10. In general, discharge  
 442 models were able to reproduce SWAT simulations for the three BMPs;  $R^2$  ranging from  
 443 0.86 to 0.9. Mean discharge simulated with the statistical equations was equal to that of  
 444 SWAT (Table 10). Mean discharge (636 mm) for the no-BMP-case (BMP 3) was greater  
 445 than that for BMPs using contour tillage and FDTs (619 and 628 mm for BMP 1 and 2,  
 446 respectively), suggesting that contour tillage and FDTs can cause evapotranspiration to  
 447 increase.

448 Models Sed1\_2 and Sed1\_3 were able to reproduce simulations with SWAT (yielding  
 449  $R^2 = 0.71$  and  $0.57$ , respectively), and simulated mean sediment loadings were close to  
 450 that of SWAT (Table 10). Models Sed1\_1 and Sed2 tended to underestimate results from  
 451 SWAT (Table 10), with an overall lower mean sediment loading of  $10.78$  vs.  $12.84$  and  
 452  $8.31$  vs.  $9.4 \text{ t ha}^{-1}$ , respectively. Mean sediment loading with Sed3 ( $0.89 \text{ t ha}^{-1}$ ) was



453 slightly greater than that of SWAT ( $0.84 \text{ t ha}^{-1}$ ), due to the fact that Sed3 only took into  
454 account TERR\_P, whereas SWAT took into account TERR\_CN and the impact of  
455 grassed waterways. Results from the statistical equations showed that the mean sediment  
456 loading for BMP 2 ( $8.31 \text{ t ha}^{-1}$ ) was significantly different than that for BMPs 1 and 3,  
457 with mean loading of  $0.89$  and  $10.78 \text{ t ha}^{-1}$  (Table 10). The smallest mean sediment  
458 loading ( $0.09 \text{ t ha}^{-1}$ ) was found to occur with the FORT land use grouping (Table 10).

459 The four  $\text{NO}_3\text{-N}$  and Sol-P loading equations explained ~50% of the variation in the  
460 SWAT simulations for the same variables, with  $R^2$  ranging from 0.33 to 0.59 (Table 10).  
461 Mean  $\text{NO}_3\text{-N}$  and Sol-P loadings with the statistical equations were all slightly less than  
462 the values produced with SWAT for the different BMPs (Table 10). Mean  $\text{NO}_3\text{-N}$   
463 loadings were greater for BMP 1 ( $44 \text{ kg ha}^{-1}$ ) than those for BMPs 2 and 3 with both  
464 giving  $39 \text{ kg ha}^{-1}$  (Table 10), due to increased infiltration with FDT. Mean Sol-P loading  
465 ( $0.8 \text{ kg ha}^{-1}$ ) was less for BMP 3 than for BMP 2 ( $0.89 \text{ kg ha}^{-1}$ ), whereas much greater  
466 than for BMP 1 ( $0.43 \text{ kg ha}^{-1}$ ). Although contour tillage can help reduce sediment loading  
467 by modifying micro-topography and reducing erosion runoff (the reason we set  $\text{USLE}_P$   
468  $< 1$ ), Sol-P transported with surface runoff increased due to reduced residue cover  
469 protecting the soil surface during winter and during the snowmelt season. When FDT was  
470 implemented with tillage, however, less surface runoff was generated due to increased  
471 infiltration leading to a reduction in Sol-P loading. Mean  $\text{NO}_3\text{-N}$  and Sol-P loadings for  
472 the FORT land grouping ( $10$  vs.  $0.06 \text{ kg ha}^{-1}$ ) were much less than those of the CRGP  
473 land grouping,  $39$  vs.  $0.8 \text{ kg ha}^{-1}$  (Table 10).



**Table 10** Comparisons of simulations of statistical models and outputs from SWAT for different land use groups and BMPs based on mean and standard deviation for the entire simulation period (1992-2011).

Variable	Index	No-BMP			Tillage			FDT + Tillage		
		CRGP		NOCR	FORT		CRGP	CRGP		FDT + Tillage
		SWAT	Fitted	SWAT	Fitted	SWAT	Fitted	SWAT	Fitted	SWAT
Discharge (mm)	Mean	→	→	636	636	←	←	619	619	628
	SD	→	→	144	133	←	←	140	132	151
	R <sup>2</sup>	→	→	0.86 (DisI)	←	←	←	0.88 (Dis2)	0.90 (Dis3)	0.90 (Dis3)
Sediment (t ha <sup>-1</sup> )	Mean	12.84	10.78	1.80	1.71	0.10	0.09	9.40	8.31	0.84
	SD	11.86	9.44	1.94	1.95	0.14	0.16	8.28	7.38	2.72
	R <sup>2</sup>	0.48 (SedI_1)	0.71 (SedI_2)	0.57 (SedI_3)	—	—	—	0.56 (Sed2)	—	—
NO <sub>3</sub> -N (kg ha <sup>-1</sup> )	Mean	43	39	24	—	10	10	43	39	47
	SD	24	14	16	—	6	3	24	14	29
	R <sup>2</sup>	0.40 (N1_1)	—	—	—	0.33 (N1_3)	—	0.39 (N2)	0.59 (N3)	—
Sol-P (kg ha <sup>-1</sup> )	Mean	0.88	0.80	0.61	—	0.08	0.06	0.98	0.89	0.49
	SD	0.49	0.32	0.46	—	0.06	0.03	0.59	0.38	0.33
	R <sup>2</sup>	0.47 (P1_1)	—	—	—	0.38 (P1_3)	—	0.48 (P2)	0.52 (P3)	—

Note: CRGP refers to crop groups including AGRL, GRAN, and GRAS; the statistics for discharge in no-BMP scenario are based on CRGP, NOCR, and FORT.

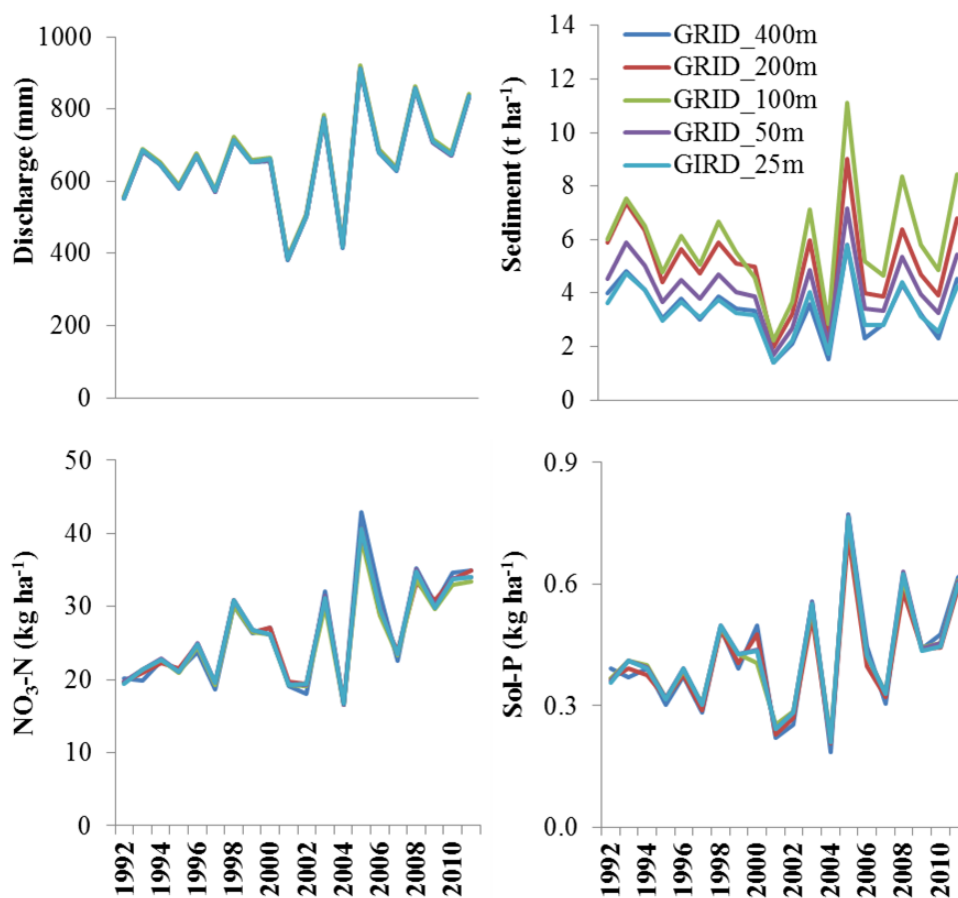




## 478     **3.2   LBAT Assessment**

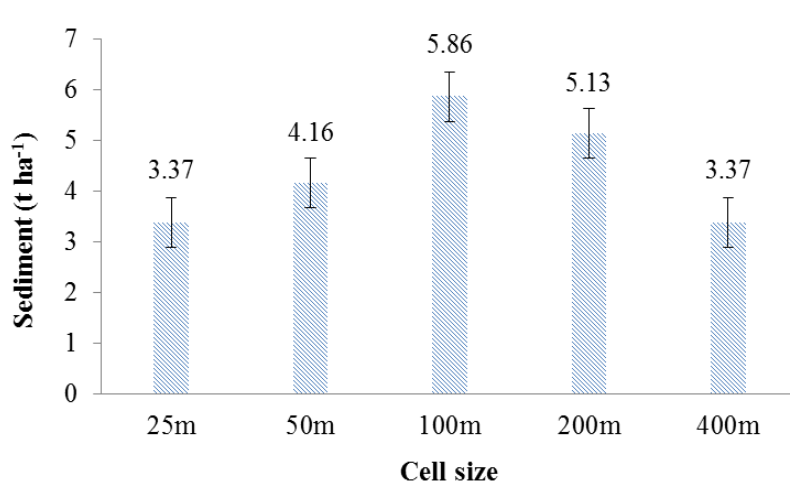
### 479     **3.2.1   Impact of Grid Cell Size on LBAT Simulation**

480         Simulations of water quantity and quality by LBAT with different grid-cell sizes (i.e.,  
481         25, 50, 100, 200, and 400 m) for BBW are shown in Fig. 4. Statistical tests indicated that  
482         grid-cell size had a significant effect on sediment loading ( $p$ -value  $< 0.01$ ), with no effect  
483         observed for discharge and  $\text{NO}_3\text{-N}$  and Sol-P loadings ( $p$ -values  $> 0.99$ ). Increasing cell  
484         size (i.e., slope length) increased sediment loading. However, the mean slope gradient  
485         was reduced. As a result, the mean sediment loadings were correlated non-linearly with  
486         cell size (Fig. 13). The highest mean sediment loading was found with a cell size of 100  
487         m ( $5.86 \text{ t ha}^{-1}$ ), whereas the lowest was found to occur with a cell size of 25 and 400 m  
488         ( $3.37 \text{ t ha}^{-1}$ ). The LBAT with a cell size of 25 and 400 m was able to generate sediment  
489         loadings consistent with field measurements. Considering computational efficiency, we  
490         chose a grid-cell size of 400 m as the basic LBAT-simulation unit for LRW.



491

492 **Fig. 4** LBAT-produced simulations of annual stream discharge and sediment,  $\text{NO}_3\text{-N}$ , and  
 493 Sol-P loadings determined for different DEM grid-cell sizes (i.e., 25, 50, 100, 200, and  
 494 400 m).



495

496 **Fig. 5** Impact of grid-cell size on LBAT-simulation of sediment loading. Mean annual  
 497 sediment loadings and standard errors (vertical bars) from 1992 to 2011 are indicated.

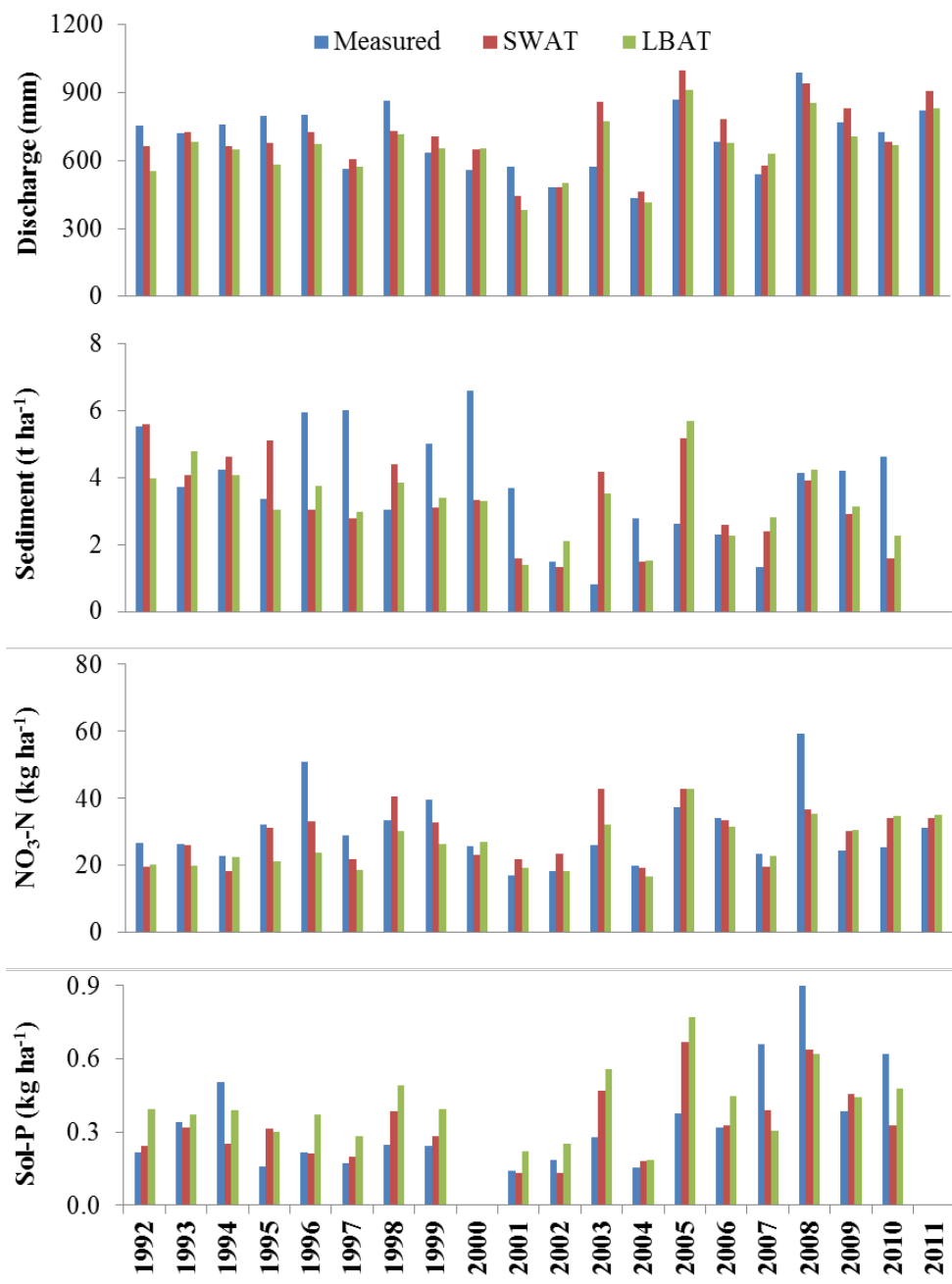
498



499

### 500 **3.2.2 LBAT vs. SWAT Applications to BBW**

501 Simulations of water quantity and quality with LBAT and SWAT are compared with  
502 field measurements from BBW (Fig. 6). Model assessments are shown in Table 11. Both  
503 LBAT and SWAT were able to capture a significant portion of the variation in measured  
504 annual stream discharge ( $R^2 = 0.48$  and  $0.56$ , respectively) and  $\text{NO}_3\text{-N}$  and Sol-P  
505 loadings ( $R^2 = 0.25$ ,  $0.32$ ,  $0.23$ , and  $0.38$ , respectively); however, this was not the case  
506 when annual sediment loading was considered (Table 11; Fig. 6) due to the fact that the  
507 current version of SWAT does not address soil erosion caused by freeze-thaw cycles (Qi  
508 et al., 2017b). Absolute values of Re with LBAT were less than 48 for these four  
509 variables (Table 11). The mean discharge and sediment loading with LBAT were slightly  
510 less than those of SWAT and field measurements, while the mean Sol-P loading ( $0.5 \text{ kg}$   
511  $\text{ha}^{-1}$ ) was greater;  $0.33$  and  $0.34 \text{ kg ha}^{-1}$  for SWAT and field measurements, respectively  
512 (Table 11). The mean  $\text{NO}_3\text{-N}$  loading ( $30 \text{ kg ha}^{-1}$ ) with LBAT was equal to the mean  
513 based on field measurements, whereas it was slightly greater than that of SWAT ( $29 \text{ kg}$   
514  $\text{ha}^{-1}$ ). These results indicated that LBAT and SWAT performed equally well in  
515 reproducing estimates of water quantity and quality at the outlet of BBW.



516

517 **Fig. 6** Simulations of annual stream discharge and sediment, NO<sub>3</sub>-N, and Sol-P loadings  
 518 with LBAT and SWAT compared with field measurements at the outlet of BBW.



519

520 **Table 11** Statistical assessments of LBAT and SWAT in simulations of annual stream  
 521 discharge and sediment, NO<sub>3</sub>-N, and Sol-P loadings at the outlet of BBW for the  
 522 simulation period of 1992-2011.

523

Variable	Index	Measured	SWAT	LBAT
Discharge (mm)	Mean	696	706	655
	Re (%)	—	2	-6
	R <sup>2</sup>	—	0.56	0.48
Sediment (t ha <sup>-1</sup> )	Mean	3.77	3.34	3.31
	Re (%)	—	-12	-12
	R <sup>2</sup>	—	0.02	0.02
NO <sub>3</sub> -N (kg ha <sup>-1</sup> )	Mean	30	29	30
	Re (%)	—	-3	0
	R <sup>2</sup>	—	0.32	0.25
Sol-P (kg ha <sup>-1</sup> )	Mean	0.34	0.33	0.50
	Re (%)	—	-3	48
	R <sup>2</sup>	—	0.38	0.23

524

525

### 526 3.2.3 LBAT vs. SWAT in LRW

527 Simulations of water quantity and quality with LBAT and the uncalibrated and  
 528 calibrated versions of SWAT are compared with field measurements for LRW (Fig. 7).  
 529 Model assessments for different simulation periods (depending on measurement  
 530 availability) are shown in Table 12. It is worth noting that, to eliminate unrealistic results,  
 531 USLE\_LS was constrained in Sed1\_2 to the NOCR land use group:

532

$$533 \quad USLE_{LS} = \begin{cases} Eq. 6-1 & USLE_{LS} \leq 1.28 \\ 1.28 & USLE_{LS} > 1.28 \end{cases} \quad (8)$$

534



535 where 1.28 is the maximum USLE\_LS for BBW.

536 In general, the two versions of SWAT and LBAT slightly underestimated annual  
537 stream discharge, capturing its variation reasonably well (Fig. 7a). The uncalibrated and  
538 calibrated versions of SWAT had the least and largest absolute values of Re (Re = -2 and  
539 -9), whereas LBAT Re = -6 (Table 12). The uncalibrated version of SWAT severely  
540 overestimated annual sediment and NO<sub>3</sub>-N loading (Re = 212 and 87, respectively; Figs.  
541 7b and c), whereas the calibrated version of SWAT and LBAT underestimated sediment  
542 loading (Re = -32 and -52, respectively) and overestimated NO<sub>3</sub>-N loading (Re = 22 and  
543 27, respectively; Table 12). In general, the calibrated version of SWAT and LBAT  
544 captured the variation in annual sediment and NO<sub>3</sub>-N loadings reasonably well (Figs. 7b  
545 and c). However, the two versions of SWAT and LBAT failed to capture the variation in  
546 annual Sol-P loadings (Fig. 7d). The LBAT had the smallest absolute value of Re (i.e., Re  
547 = -16), while the uncalibrated and calibrated versions of SWAT had larger values (Re = -  
548 59 and -55, respectively). These results suggested that the LBAT and the calibrated  
549 version of SWAT performed equally well in simulating annual stream flow and sediment  
550 and NO<sub>3</sub>-N loadings, with LBAT performing slightly better for annual Sol-P loading.  
551 LBAT performed noticeably better than the uncalibrated version of SWAT, especially for  
552 annual sediment and NO<sub>3</sub>-N loadings.

553

554

555

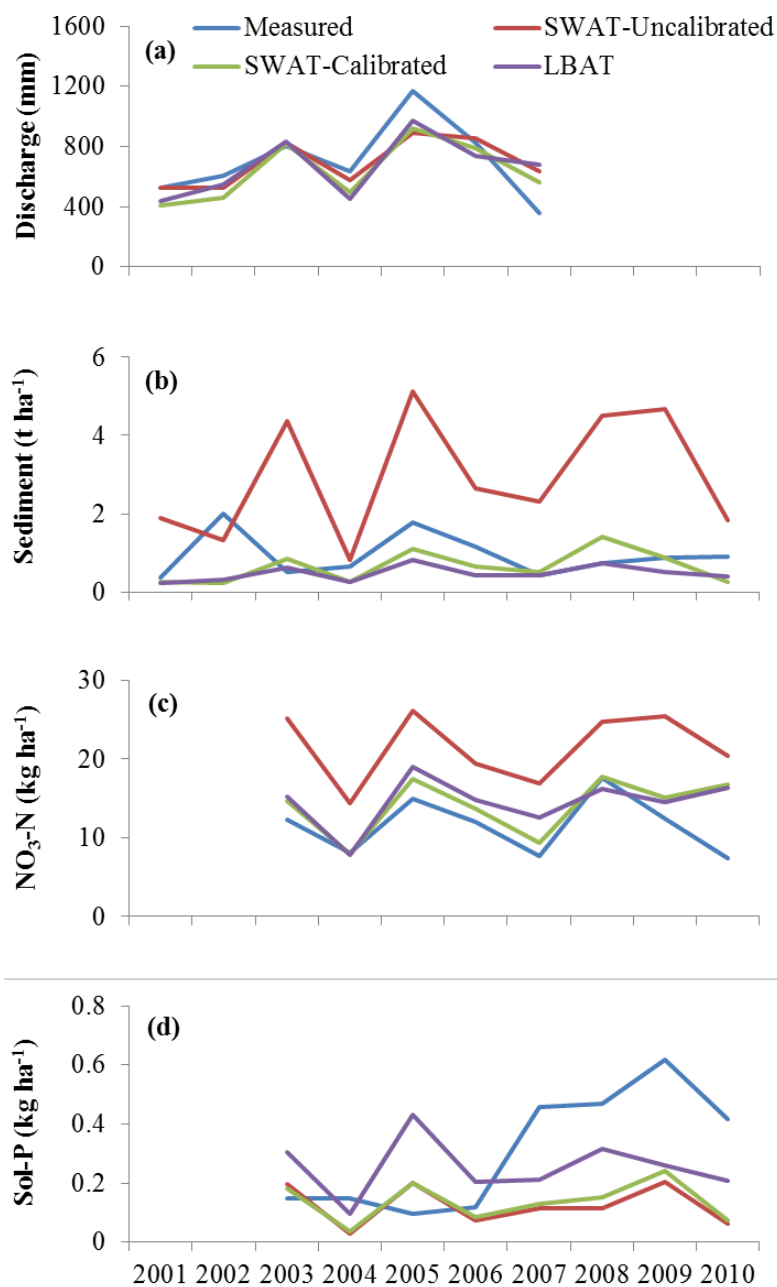


**Table 12** Statistical assessments of LBAT and SWAT for annual stream discharge and sediment, NO<sub>3</sub>-N, and Sol-P loadings at the outlet of LRW for different simulation periods

Period	Variable	Index	Measurement	SWAT -Uncalibrated	SWAT -Calibrated	LBAT
01-07	Discharge (mm)	Mean	704	691	638	559
		Re (%)	—	-2	-9	-6
01-10	Sediment (t ha <sup>-1</sup> )	Mean	0.95	2.95	0.65	561
		Re (%)	—	212	-32	-52
03-10	NO <sub>3</sub> -N (kg ha <sup>-1</sup> )	Mean	12	22	14	562
		Re (%)	—	87	22	27
03-10	Sol-P (kg ha <sup>-1</sup> )	Mean	0.31	0.13	0.14	0.26
		Re (%)	—	-59	-55	564

Since LBAT is based on decision rules (statistical equations) which were derived from SWAT simulations for BBW, its usage should be constrained to areas with soil, landscape, and land use characteristics similar to BBW. Input characteristics exceeding the range of SWAT data considered could lead to large errors in predictions. LBAT is flexible in its structure, and with thoughtful development of internal rules, it can be applied to diverse environments.





572

573 **Fig. 7** Simulations of annual stream discharge and sediment,  $\text{NO}_3\text{-N}$ , and Sol-P loadings

574 with LBAT and SWAT compared with field measurements at the outlet of LRW.



575

#### 576 **3.2.4 FDT Assessment in LRW**

577 Mean annual water quantity and quality simulated with LBAT for agricultural lands of  
 578 LRW are shown in Table 13. The mean annual discharge for the baseline scenario was  
 579 626 mm greater than that for the six FDT scenarios (Table 13). When all agricultural  
 580 lands were protected (S6), there was a 2% reduction in discharge (equivalent to 11 mm;  
 581 Table 13). With the steepest areas protected (accounting for 10% of the total land base;  
 582 S1), the mean annual sediment loading was reduced by as much as 43% (equivalent to  
 583 4.5 t ha<sup>-1</sup>; Table 13) and by as much as 81% (i.e., 8.57 t ha<sup>-1</sup>) with all agricultural lands  
 584 protected (S6; Table 13). Mean annual Sol-P loading was reduced by 51% (equivalent to  
 585 0.47 kg ha<sup>-1</sup>; Table 13). In contrast, increased usage of FDT tended to increase the mean  
 586 annual loading of NO<sub>3</sub>-N, by about 6% when used across all agricultural lands  
 587 (equivalent to 1.73 kg ha<sup>-1</sup>).

588

589

590

591

592

593

594

595

596



**Table 6.13** Impact of FDT on mean annual discharge and sediment, NO<sub>3</sub>-N, and Sol-P loadings simulated with LBAT under different FDT, provided in Table 3.

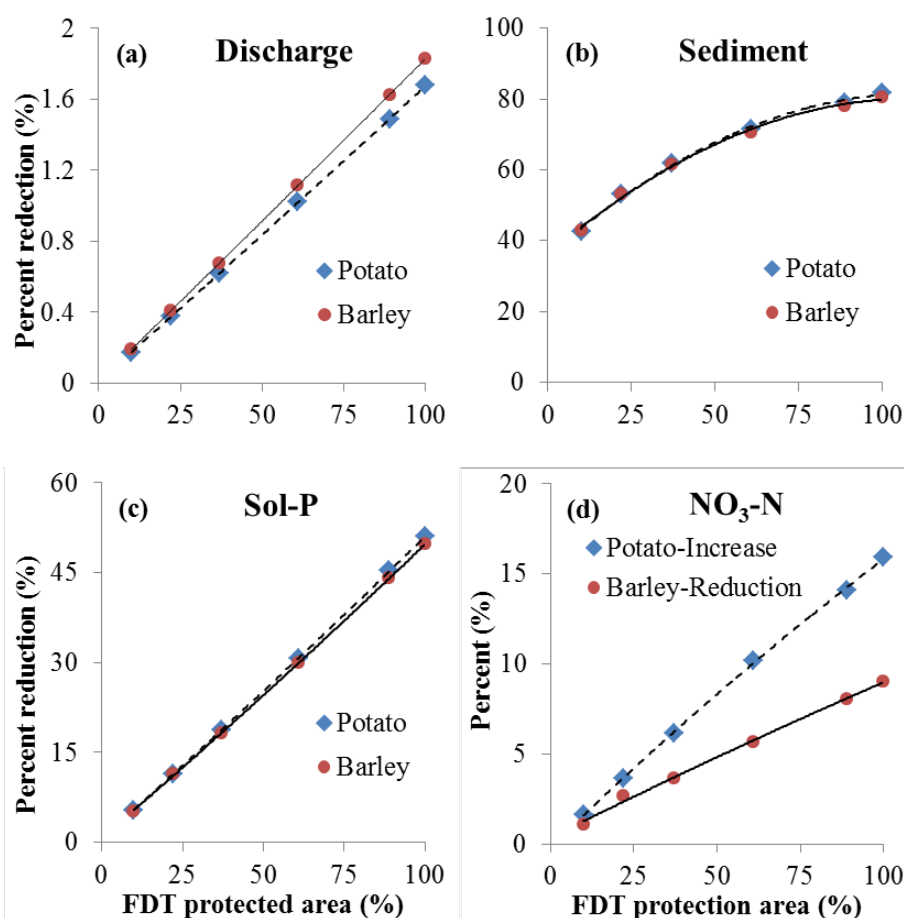
Variable	Index	Baseline	S1	S2	S3	S4	S5	S6
Discharge (mm)	Mean	626	625	623	622	619	616	615
	MD	—	-1	-2	-4	-7	-10	-11
	PRD (%)	—	0	0	-1	-1	-2	-2
Sediment (t ha <sup>-1</sup> )	Mean	10.54	6.04	4.94	4.02	3.04	2.26	1.97
	MD	—	-4.50	-5.60	-6.52	-7.50	-8.28	-8.57
	PRD (%)	—	-43	-53	-62	-71	-79	-81
NO <sub>3</sub> -N (kg ha <sup>-1</sup> )	Mean	29.70	29.86	30.02	30.34	30.82	31.22	31.42
	MD	—	0.16	0.32	0.64	1.13	1.52	1.73
	PRD (%)	—	1	1	2	4	5	6
Sol-P (kg ha <sup>-1</sup> )	Mean	0.94	0.89	0.83	0.76	0.65	0.52	0.46
	MD	—	-0.05	-0.11	-0.17	-0.28	-0.42	-0.47
	PRD (%)	—	-5	-11	-19	-30	-45	-51

Percentage change (based on PRD) of water quantity and quality were plotted against percentage area of FDT for potato and barley in Fig. 8. Increasing the usage of FDT helped to reduce discharge and sediment and Sol-P loadings for both crop types (Figs. 8a, b, and c). It is worth noting that sediment loading decreased with increasing usage of FDT (Fig. 16b). An opposite trend was observed for potato and barley with respect to the impact of FDT on NO<sub>3</sub>-N loading. With the increased usage of FDT, NO<sub>3</sub>-N loadings increased linearly for potato, while it decreased for barley. The increased for potato was nearly twice as much as the reduction for barley (Fig. 16d). Seemingly the interaction between barley and FDT had positive impacts on nitrate retention in soils, whereas the interaction between potato and FDT had an opposite effect.

These results are consistent with the results from previous studies (Yang et al., 2012; Yang et al., 2010), which used SWAT to assess the impact of FDT on water quantity and quality within BBW. When using SWAT, greater efforts are needed to prepare basic



613 inputs, such as daily weather records, to proceed with its calibration and validation,  
 614 involving complex scenario setup and analysis. For every new watershed, SWAT needs  
 615 dedicated effort and time for its setup. LBAT, in contrast, can be used for multiple  
 616 watersheds as long as they have similar environmental conditions. Scenario analysis can  
 617 be directly conducted with different combinations of land use and BMPs using fewer  
 618 inputs than what is required by SWAT. Also, once developed, LBAT does not require  
 619 additional calibration.



621 **Fig. 8** Percentage change in discharge and sediment, NO<sub>3</sub>-N, and Sol-P loadings as a  
 622 function of % area, where FDT's were used.



#### 4. Conclusion

The present study addresses the development of a decision support tool to assess the impact of land use change and BMPs on water quantity and quality for large ungauged watersheds. An enhanced version of SWAT was calibrated and validated for an experimental watershed. Multiple regression analyses were used to develop statistical equations based on simulations from SWAT. In total, three discharge and five sediment,  $\text{NO}_3\text{-N}$ , and Sol-P loading models were developed for different combinations of land use groups and BMP scenarios. Only four common predictors (i.e., annual precipitation, annual mean air temperature, mean saturated hydraulic conductivity of soil, and land use groups) and three unique predictors (LS-factor and annual nitrogen and phosphorus application rates for sediment,  $\text{NO}_3\text{-N}$ , and Sol-P loading models, respectively) are required.

With the aid of ArcGIS, statistical equations were integrated into the decision support tool, i.e., the land use and BMPs assessment tool (LBAT), whose basic simulation units are the DEM-grid cell. The LBAT was used to simulate annual water flow and sediment and nutrient loadings at the outlet of BBW. These simulations were compared with those of SWAT. LBAT and SWAT perform equally well. LBAT was subsequently applied to a large watershed (LRW). Results indicate that LBAT and the calibrated version of SWAT perform well with respect to annual stream discharge and sediment and  $\text{NO}_3\text{-N}$  loadings. LBAT performed slightly better, when Sol-P loading was considered. Compared with the uncalibrated version of SWAT, LBAT performed better. The impact of FDT on water quantity and quality was evaluated with LBAT for LRW; its results were consistent with the results generated with SWAT for the same region in previous studies. LBAT has



fewer input requirements than SWAT, and can be applied to multiple watersheds without additional calibration. Also, scenario analyses can be directly conducted with LBAT without complex setup procedures. We recommend using LBAT for economic analysis and management decision making for watersheds with similar environmental conditions of New Brunswick. The LBAT developed in this study may not be directly applied to other regions; however, the approach in developing LBAT can be applied to other regions of the world because of its flexible structure.

#### **Acknowledgement**

The funding support for this project was provided by Agriculture and Agri-Food Canada (AAFC) through project #1145, entitled “Integrating selected BMPs to maximize environmental and economic benefits at the field and watershed scales for sustainable potato production in New Brunswick”, and Natural Science and Engineering Research Council (NSERC) through Discovery Grants to both CPAB and FRM. The research is also partially supported by NASA (NNX17AE66G) and USDA (2017-67003-26485). Authors are thankful to S. Lavoie, J. Monteith, and L. Stevens for their technical support in data collection and sample analyses.

#### **References**

Arnold, J.G., Srinivasan, R., Muttiah, R.S., Williams, J.R., 1998. Large area hydrologic modeling and assessment part I: Model development. JAWRA Journal of the American Water Resources Association 34(1) 73-89.



- 668 Beasley, D., Huggins, L., Monke, a., 1980. ANSWERS: A model for watershed planning.  
669 Transactions of the ASAE 23(4) 938-0944.
- 670 Beaulac, M.N., Reckhow, K.H., 1982. An Examination of Land Use-Nutrient Export  
671 Relationships. JAWRA Journal of the American Water Resources Association  
672 18(6) 1013-1024.
- 673 Behera, S., Panda, R., 2006. Evaluation of management alternatives for an agricultural  
674 watershed in a sub-humid subtropical region using a physical process based  
675 model. Agriculture, Ecosystems & Environment 113(1) 62-72.
- 676 Blöschl, G., Grayson, R., 2001. Spatial observations and interpolation. Spatial patterns in  
677 catchment hydrology: observations and modelling, edited by: Grayson, R. and  
678 Blöschl, G., Cambridge University Press, UK, ISBN 0-521-63316-8 17-50.
- 679 Blöschl, G., Sivapalan, M., 1995. Scale issues in hydrological modelling: a review.  
680 Hydrological Processes 9(3-4) 251-290.
- 681 Borah, D., Bera, M., 2003. Watershed-scale hydrologic and nonpoint-source pollution  
682 models: Review of mathematical bases. Transactions of the ASAE 46(6) 1553.
- 683 Borah, D.K., Bera, M., 2004. Watershed-scale hydrologic and nonpoint-source pollution  
684 models: Review of applications. Transactions of the ASAE 47(3) 789-803.
- 685 Borah, D.K., Demissie, M., Keefer, L.L., 2002. AGNPS-based assessment of the impact  
686 of BMPs on nitrate-nitrogen discharging into an Illinois water supply lake. Water  
687 International 27(2) 255-265.
- 688 Chow, L., Xing, Z., Benoy, G., Rees, H., Meng, F., Jiang, Y., Daigle, J., 2011. Hydrology  
689 and water quality across gradients of agricultural intensity in the Little River



- 690 watershed area, New Brunswick, Canada. Journal of Soil and Water conservation  
691 66(1) 71-84.
- 692 Chow, T., Rees, H., 2006. Impacts of intensive potato production on water yield and  
693 sediment load (Black Brook Experimental Watershed: 1992–2002 summary).  
694 Potato Research Centre, AAFC, Fredericton, p. 26.
- 695 D'Arcy, B., Frost, A., 2001. The role of best management practices in alleviating water  
696 quality problems associated with diffuse pollution. Science of the Total  
697 Environment 265(1) 359-367.
- 698 Endreny, T.A., Wood, E.F., 2003. WATERSHED WEIGHTING OF EXPORT  
699 COEFFICIENTS TO MAP CRITICAL PHOSPHOROUS LOADING AREAS1.  
700 Wiley Online Library.
- 701 Gassman, P.W., Reyes, M.R., Green, C.H., Arnold, J.G., 2005. SWAT peer-reviewed  
702 literature: a review, 3rd International SWAT Conference. Zurich, Switzerland.
- 703 Ihaka, R., Gentleman, R., 1996. R: a language for data analysis and graphics. Journal of  
704 computational and graphical statistics 5(3) 299-314.
- 705 Keselman, H., Huberty, C.J., Lix, L.M., Olejnik, S., Cribbie, R.A., Donahue, B.,  
706 Kowalchuk, R.K., Lowman, L.L., Petoskey, M.D., Keselman, J.C., 1998.  
707 Statistical practices of educational researchers: An analysis of their ANOVA,  
708 MANOVA, and ANCOVA analyses. Review of Educational Research 68(3) 350-  
709 386.
- 710 Knisel, W.G., 1980. CREAMS: a field scale model for Chemicals, Runoff, and Erosion  
711 from Agricultural Management Systems [USA]. United States. Dept. of  
712 Agriculture. Conservation research report (USA).





- 713 Leonard, R., Knisel, W., Still, D., 1987. GLEAMS: Groundwater loading effects of  
714 agricultural management systems. Transactions of the ASAE 30(5) 1403-1418.
- 715 Li, Q., Qi, J., Xing, Z., Li, S., Jiang, Y., Danieleescu, S., Zhu, H., Wei, X., Meng, F.-R.,  
716 2014. An approach for assessing impact of land use and biophysical conditions  
717 across landscape on recharge rate and nitrogen loading of groundwater.  
718 Agriculture, Ecosystems & Environment 196 114-124.
- 719 Liu, Y., Yang, W., Yu, Z., Lung, I., Gharabaghi, B., 2015. Estimating sediment yield  
720 from upland and channel erosion at a watershed scale using SWAT. Water  
721 resources management 29(5) 1399-1412.
- 722 Marshall, I., Schut, P., Ballard, M., 1999. A national ecological framework for Canada:  
723 Attribute data. Ottawa, Ontario: Environmental Quality Branch, Ecosystems  
724 Science Directorate, Environment Canada and Research Branch. Agriculture and  
725 Agri-Food Canada.
- 726 May, L., Place, C., 2010. A GIS-based model of soil erosion and transport, Freshwater  
727 Forum.
- 728 Mellerowicz, K.T., 1993. Soils of the Black Brook Watershed St. Andre Parish,  
729 Madawaska County, New Brunswick. [Fredericton]: New Brunswick Department  
730 of Agriculture.
- 731 Mostaghimi, S., Park, S., Cooke, R., Wang, S., 1997. Assessment of management  
732 alternatives on a small agricultural watershed. Water research 31(8) 1867-1878.
- 733 Novara, A., Gristina, L., Saladino, S., Santoro, A., Cerdà, A., 2011. Soil erosion  
734 assessment on tillage and alternative soil managements in a Sicilian vineyard. Soil  
735 and Tillage Research 117 140-147.



- 736 Ongley, E.D., Xiaolan, Z., Tao, Y., 2010. Current status of agricultural and rural non-  
737 point source pollution assessment in China. *Environmental Pollution* 158(5) 1159-  
738 1168.
- 739 Panagopoulos, Y., Makropoulos, C., Mimikou, M., 2011. Reducing surface water  
740 pollution through the assessment of the cost-effectiveness of BMPs at different  
741 spatial scales. *Journal of environmental management* 92(10) 2823-2835.
- 742 Pimentel, D., Krummel, J., 1987. Biomass energy and soil erosion: Assessment of  
743 resource costs. *Biomass* 14(1) 15-38.
- 744 Qi, J., Li, S., Jamieson, R., Hebb, D., Xing, Z., Meng, F.-R., 2017a. Modifying SWAT  
745 with an energy balance module to simulate snowmelt for maritime regions.  
746 *Environmental Modelling & Software* 93 146-160.
- 747 Qi, J., Li, S., Li, Q., Xing, Z., Bourque, C.P.-A., Meng, F.-R., 2016a. Assessing an  
748 enhanced version of SWAT on water quantity and quality simulation in regions  
749 with seasonal snow cover. *Water Resources Management* 1-17.
- 750 Qi, J., Li, S., Li, Q., Xing, Z., Bourque, C.P.-A., Meng, F.-R., 2016b. A new soil-  
751 temperature module for SWAT application in regions with seasonal snow cover.  
752 *Journal of hydrology* 538 863-877.
- 753 Qi, J., Li, S., Yang, Q., Xing, Z., Meng, F.-R., 2017b. SWAT setup with long-term  
754 detailed landuse and management records and modification for a micro-watershed  
755 influenced by freeze-thaw cycles. *Water Resources Management*. DOI  
756 10.1007/s11269-017-1718-2



- 757 Quan, W., Yan, L., 2001. Effects of agricultural non-point source pollution on  
758 eutrophication of water body and its control measure. *Acta Ecologica Sinica*  
759 22(3) 291-299.
- 760 Reckhow, K., Simpson, J., 1980. A procedure using modeling and error analysis for the  
761 prediction of lake phosphorus concentration from land use information. *Canadian*  
762 *Journal of Fisheries and Aquatic Sciences* 37(9) 1439-1448.
- 763 Renschler, C., Lee, T., 2005. Spatially distributed assessment of short-and long-term  
764 impacts of multiple best management practices in agricultural watersheds. *Journal*  
765 *of Soil and Water conservation* 60(6) 446-456.
- 766 Renschler, C.S., Harbor, J., 2002. Soil erosion assessment tools from point to regional  
767 scales—the role of geomorphologists in land management research and  
768 implementation. *Geomorphology* 47(2) 189-209.
- 769 Sadeghi, S.H., Moosavi, V., Karami, A., Behnia, N., 2012. Soil erosion assessment and  
770 prioritization of affecting factors at plot scale using the Taguchi method. *Journal*  
771 *of hydrology* 448 174-180.
- 772 Sharpley, A.N., Williams, J.R., 1990. EPIC-erosion/productivity impact calculator: 1.  
773 Model documentation. Technical Bulletin-United States Department of  
774 Agriculture(1768 Pt 1).
- 775 Singh, V.P., 1995. Computer models of watershed hydrology. Water Resources  
776 Publications.
- 777 Singh, V.P., Frevert, D.K., 2005. Watershed Models. CRC Press, Boca Raton, FL, USA.
- 778 Singh, V.P., Woolhiser, D.A., 2002. Mathematical modeling of watershed hydrology.  
779 *Journal of hydrologic engineering* 7(4) 270-292.



- 780 Turkelboom, F., Poesen, J., Ohler, I., Van Keer, K., Ongprasert, S., Vlassak, K., 1997.  
781 Assessment of tillage erosion rates on steep slopes in northern Thailand.  
782 CATENA 29(1) 29-44.
- 783 Ullrich, A., Volk, M., 2009. Application of the Soil and Water Assessment Tool (SWAT)  
784 to predict the impact of alternative management practices on water quality and  
785 quantity. *Agricultural Water Management* 96(8) 1207-1217.
- 786 Urbonas, B., 1994. Assessment of stormwater BMPs and their technology. *Water Science*  
787 *and Technology* 29(1-2) 347-353.
- 788 Vanoni, V.A., 1975. *Sedimentation Engineering: American Society of Civil Engineers,*  
789 *Manuals and Reports on Engineering Practice.*
- 790 Veldkamp, A., Lambin, E.F., 2001. Predicting land-use change. *Agriculture, Ecosystems*  
791 *& Environment* 85(1) 1-6.
- 792 Viavattene, C., Scholes, L., Revitt, D., Ellis, J., 2008. A GIS based decision support  
793 system for the implementation of stormwater best management practices, 11th  
794 International Conference on Urban Drainage, Edinburgh, Scotland, UK.
- 795 Vörösmarty, C.J., McIntyre, P.B., Gessner, M.O., Dudgeon, D., Prusevich, A., Green, P.,  
796 Glidden, S., Bunn, S.E., Sullivan, C.A., Liermann, C.R., 2010. Global threats to  
797 human water security and river biodiversity. *Nature* 467(7315) 555-561.
- 798 Wilson, C.J., Carey, J.W., Beeson, P.C., Gard, M.O., Lane, L.J., 2001. A GIS-based  
799 hillslope erosion and sediment delivery model and its application in the Cerro  
800 Grande burn area. *Hydrological Processes* 15(15) 2995-3010.
- 801 Xing, Z., Chow, L., Rees, H., Meng, F., Li, S., Ernst, B., Benoy, G., Zha, T., Hewitt,  
802 L.M., 2013. Influences of sampling methodologies on pesticide-residue detection



- 803 in stream water. Archives of environmental contamination and toxicology 64(2)  
804 208-218.
- 805 Yan, B., Fang, N., Zhang, P., Shi, Z., 2013. Impacts of land use change on watershed  
806 streamflow and sediment yield: an assessment using hydrologic modelling and  
807 partial least squares regression. Journal of hydrology 484 26-37.
- 808 Yang, Q., Benoy, G.A., Chow, T.L., Daigle, J.-L., Bourque, C.P.-A., Meng, F.-R., 2012.  
809 Using the Soil and Water Assessment Tool to estimate achievable water quality  
810 targets through implementation of beneficial management practices in an  
811 agricultural watershed. Journal of environmental quality 41(1) 64-72.
- 812 Yang, Q., Meng, F.-R., Zhao, Z., Chow, T.L., Benoy, G., Rees, H.W., Bourque, C.P.-A.,  
813 2009. Assessing the impacts of flow diversion terraces on stream water and  
814 sediment yields at a watershed level using SWAT model. Agriculture, Ecosystems  
815 & Environment 132(1) 23-31.
- 816 Yang, Q., Zhao, Z., Benoy, G., Chow, T.L., Rees, H.W., Bourque, C.P.-A., Meng, F.-R.,  
817 2010. A watershed-scale assessment of cost-effectiveness of sediment abatement  
818 with flow diversion terraces. Journal of environmental quality 39(1) 220-227.
- 819 Young, R.A., Onstad, C., Bosch, D., Anderson, W., 1989. AGNPS: A nonpoint-source  
820 pollution model for evaluating agricultural watersheds. Journal of Soil and Water  
821 conservation 44(2) 168-173.
- 822 Zhang, W., Wu, S., Ji, H., Kolbe, H., 2004. Estimation of agricultural non-point source  
823 pollution in China and the alleviating strategies I. Estimation of agricultural non-  
824 point source pollution in China in early 21 century. Scientia agricultura sinica  
825 37(7) 1008-1017.



826 Zhao, Z., Benoy, G., Chow, T.L., Rees, H.W., Daigle, J.-L., Meng, F.-R., 2010. Impacts  
827 of accuracy and resolution of conventional and LiDAR based DEMs on  
828 parameters used in hydrologic modeling. Water resources management 24(7)  
829 1363-1380.

830 Zhao, Z., Chow, T.L., Yang, Q., Rees, H.W., Benoy, G., Xing, Z., Meng, F.-R., 2008.  
831 Model prediction of soil drainage classes based on digital elevation model  
832 parameters and soil attributes from coarse resolution soil maps. Canadian Journal  
833 of Soil Science 88(5) 787-799.

834

835